

One and two-photon detachment cross-sections of Ps^-

K. Maniadaki¹, L.A.A. Nikolopoulos^{2,a}, and P. Lambropoulos^{1,2}

¹ Department of Physics, University of Crete, Heraklion-Crete 71110, Greece

² Institute of Electronic Structure and Laser, FORTH, P.O. Box 1527, Heraklion-Crete 71110, Greece

Received 24 January 2002 / Received in final form 9 April 2002

Published online 19 July 2002 – © EDP Sciences, Società Italiana di Fisica, Springer-Verlag 2002

Abstract. We present detailed calculations for one- and two-photon above-threshold detachment (ATD) cross-sections of the negative positronium ion $\text{Ps}^- (e^+e^-e^-)$, below the threshold of $\text{Ps}(n=2)$, using a configuration interaction (CI) method on a B splines basis. Both the one- and two-photon detachment cross-sections have a form similar to the corresponding spectra of the H^- ion, scaled accordingly. The peak value of the one-photon cross-section agrees very well with the calculations by Bathia and Drachman [1], while it differs from those by Igarashi *et al.* [2], which give a value of 15% lower. Two-photon detachment cross-sections are also reported.

PACS. 32.80.Rm Multiphoton ionization and excitation to highly excited states (*e.g.*, Rydberg states) – 32.80.-t Photon interactions with atoms – 36.10.Dr Positronium, muonium, muonic atoms and molecules

1 Introduction

The negative positronium ion represents a rather extreme case of the pure three-body Coulomb problem. Helium and H^- , the two other fundamental cases of this problem, are objects of continuing attention as they provide a valuable testing ground for the theoretical and experimental study of the rich variety of phenomena associated with this problem. Over the years, new dimensions of the problem have been explored, particularly in helium, in the context of strong field phenomena. All along, an ongoing search for and development of new theoretical tools, purely quantum mechanical, semiclassical, or even fully classical is underway. He and H^- place different demands on a method, since the first is a compact object involving, however, long Coulomb tails, while H^- is more extended, weakly bound with correlation in the ground state being far more crucial to its existence in the first place. Ps^- represents an even more extreme case in that direction, with the added complication of a new term in the Hamiltonian owing to the fact that there is no heavy nucleus (center of mass).

Our motivation for undertaking the work that led to the results presented in this paper came from related work by other authors [1–6] and our interest in testing new methods that we have been developing and applying to a variety of problems. The experimental interest in Ps is well established. To the best of our knowledge, Ps^- for the moment represents an interesting theoretical problem and

it is in that spirit that we present our results. Presumably, some day it may also be investigated experimentally.

In order to provide an extensive exploration of the techniques we use, we have first calculated the basic quantities such as eigenenergies and photodetachment cross-sections, which have also been calculated by other authors. Then we have, in addition, calculated two-photon detachment cross-sections which explore different aspects of the system. Atomic units are used throughout this work.

2 Theory

2.1 Atomic basis

For two-electron atoms, independent-particle-type coordinates $(\mathbf{r}_1, \mathbf{r}_2)$ are usually used, where \mathbf{r}_1 represents the position vector of electron 1 relative to the nucleus, and \mathbf{r}_2 represents that of electron 2. The full Hamiltonian in these coordinates is,

$$H = -\frac{1}{2\mu}\nabla_1^2 - \frac{1}{2\mu}\nabla_2^2 - \frac{1}{M}\nabla_1 \cdot \nabla_2 - \frac{Z}{r_1} - \frac{Z}{r_2} + \frac{1}{r_{12}}, \quad (1)$$

where μ is the reduced mass of the electron-nucleus pair, M the mass of the nucleus and Z is the nuclear charge. In the usual case of a heavy nucleus (as in the case of H^-) $1/M$ is small, and this term may be neglected or treated in perturbation theory. But when the three particles are of comparable masses, as is the case of Ps^- , the cross term $-(1/M)\nabla_1 \cdot \nabla_2$ is as important as the other two terms of

^a e-mail: nlambros@iesl.forth.gr

the kinetic energy and it must be included in the calculations. An additional difference between H^- and Ps^- is that the reduced mass $\mu = M/(1+M)$ is $\mu = 1$ in the case of H^- , whereas in the case of Ps^- it is $\mu = 1/2$. This has of course been taken into account in the treatment that follows. Thus, we consider for the Ps^- , $\mu = 1/2$, $M = 1$ and $Z = 1$.

The negative positronium eigenstates satisfy the eigenvalue equation,

$$[h^{Ps}(\mathbf{r}_1) + h^{Ps}(\mathbf{r}_2) + V(\mathbf{r}_1, \mathbf{r}_2)] \Phi_{n(E)}^{SL}(\mathbf{r}_1, \mathbf{r}_2) = E_n^{SL} \Phi_{n(E)}^{SL}(\mathbf{r}_1, \mathbf{r}_2), \quad (2)$$

where E_n^{SL} is the total energy of the system, $\Phi_{n(E)}^{SL}(\mathbf{r}_1, \mathbf{r}_2)$ the LS-uncoupled two-electron state, and $h^{Ps}(\mathbf{r}_i)$, $i = 1, 2 \dots$ the positronium Hamiltonian operator, namely:

$$h^{Ps}(\mathbf{r}_i) = -\nabla_i^2 - \frac{1}{r_i} \quad (3)$$

and $V(\mathbf{r}_1, \mathbf{r}_2)$ the electron-electron interaction operator,

$$V(\mathbf{r}_1, \mathbf{r}_2) = -\nabla_1 \cdot \nabla_2 + \frac{1}{r_{12}}, \quad (4)$$

consisting of the ‘‘mass’’ polarization term $\nabla_1 \cdot \nabla_2$ and the Coulomb interaction term $1/r_{12} = 1/|\mathbf{r}_1 - \mathbf{r}_2|$. In order to solve equation (2), we expand the two-electron eigenstates $\Phi_{n(E)}^{SL}(\mathbf{r}_1, \mathbf{r}_2)$ in the basis of two-electron orbitals $\Psi_{n_1 l_1, n_2 l_2}^{SL}(\mathbf{r}_1, \mathbf{r}_2)$ [7]:

$$\Phi_{n(E)}^{SL}(\mathbf{r}_1, \mathbf{r}_2) = \sum_{n_1 l_1, n_2 l_2} C_{n(E)}^{SL}(n_1 l_1, n_2 l_2) \Psi_{n_1 l_1, n_2 l_2}^{SL}(\mathbf{r}_1, \mathbf{r}_2), \quad (5)$$

where $C_{n(E)}^{SL}(n_1 l_1, n_2 l_2)$ is an eigenvector of the Hamiltonian matrix for the n th energy eigenvalue. Here $|C_{n(E)}^{SL}(n_1 l_1, n_2 l_2)|^2$ is the probability density for the configuration $(n_1 l_1, n_2 l_2)$ in the n th energy eigenstate. When $E \leq 0$, $\Phi_{n(E)}^{SL}$ represents a bound state of energy E , indexed by the integer $n \rightarrow n(E)$, while $E > 0$ corresponds to continuum states of the system. The two-electron orbital wavefunctions $\Psi_{n_1 l_1, n_2 l_2}^{SL}(\mathbf{r}_1, \mathbf{r}_2)$ are LS-coupled, antisymmetrized products of the one-electron target radial functions $P_{nl}(r)$. Considering that the solutions of the one-electron Hamiltonian are positronium orbitals of the type:

$$\phi_{nlmm_s}(\mathbf{r}) = \frac{P_{nl}(r)}{r} Y_{lm}(\theta, \phi) \sigma(m_s) \quad (6)$$

the radial functions $P_{nl}(r)$ satisfy the equation [8]:

$$\left[-\frac{d^2}{dr^2} - \frac{1}{r} + \frac{l(l+1)}{r^2} \right] P_{nl}(r) = \epsilon_{nl} P_{nl}(r), \quad (7)$$

with ϵ_{nl} being the eigenvalue. The $P_{nl}(r)$ functions with negative or positive eigenvalues are expanded in terms of a set of B-splines of order k and total number N defined in the finite interval $[0, R]$. This way, we lead to

a generalized matrix equation for the expansion coefficients, where a simple diagonalization is performed [9–11]. The negative-energy solutions correspond to bound one-electron orbitals, while the positive-energy solutions correspond to discrete continuum eigenstates, all normalized to unity.

2.2 Structure

2.2.1 Ground state

For the calculation of one-photon detachment, the order of B-splines was $k = 9$ with $N_b = 42$ and $R = 150$. The knot sequence that we have used was sine-like, first used by Tang and Chang [9] in calculations of multiphoton processes. The total number of configurations for the symmetries $L = 0, 1, 2$ was about 2000 and the maximum number of one-electron partial waves l_1, l_2 was 4. With these parameters the value of the ground state differs by about 1% in most of our calculations from the most accurate value $E = -0.262005070232957$ to date [15]. In contrast of the negative hydrogen case, where with a similar in size basis would have cover only 90% of the ground state energy value, sufficient accuracy in the ground state of negative positronium is achieved. This is due to the extra term $-\nabla_1 \cdot \nabla_2$, appearing in the negative positronium Hamiltonian, which is opposite in sign to the ‘‘traditional’’ $1/r_{12}$ CI term. For example, the two-electron wavefunctions for the S symmetry are constructed including configurations of the type $(ns)^2, (np)^2, (nd)^2, (nf)^2, (ng)^2$ with $n = 1, 2, \dots, 60$. The matrix elements of the CI terms (see Eq. (4)) $1/r_{12}$ and $-\nabla_1 \cdot \nabla_2$ between the two-electron orbitals $\Psi_{1s^2}^{L=0}, \Psi_{2p^2}^{L=0}$ are, $\langle 1s^2 | 1/r_{12} | 2p^2 \rangle = 0.05913$ and $\langle 1s^2 | -\nabla_1 \cdot \nabla_2 | 2p^2 \rangle = -0.06758$, respectively. In the case of negative hydrogen, the latter term (mass polarization) is insignificant compared to $1/r_{12}$ (Coulombic) term. This holds for any matrix element between non-equivalent configurations. The same matrix elements between equivalent configurations is zero for the mass polarization term, due to angular momentum selection rules, while is not vanishing for the $1/r_{12}$ term.

2.2.2 Continuum states

The discrete continuum state function $\Phi_{n(E)}^{SL}(\mathbf{r}_1, \mathbf{r}_2)$, corresponding to total energy E , above the first ionization threshold, is constituted by a series of doubly excited autodetachment states embedded in the single continuum open channel $1sl$, which formally, can be separated in two parts:

$$\Phi_{n(E)}^{SL}(\mathbf{r}_1, \mathbf{r}_2) = \phi_{E,1sl}^{SL}(\mathbf{r}_1, \mathbf{r}_2) + \sum_{n_0 l_0 l'} \phi_{E,n_0 l_0 l'}^{SL}(\mathbf{r}_1, \mathbf{r}_2), \quad (8)$$

where $\phi_{E,1sl}^{SL}(\mathbf{r}_1, \mathbf{r}_2)$ represents the ionization channel and $\phi_{E,n_0 l_0 l'}^{SL}(\mathbf{r}_1, \mathbf{r}_2)$ the total contribution from all closed

channels. The ionization channel, by inspecting equation (5) is the sum of all the $1sl$ configuration series,

$$\phi_{E,1sl}^{\text{SL}}(\mathbf{r}_1, \mathbf{r}_2) = \sum_n C_E^{\text{SL}}(1s, nl) \Psi_{1s,nl}^{\text{SL}}(\mathbf{r}_1, \mathbf{r}_2), \quad (9)$$

which may be expressed in the form of a Slater determinant $\phi_{1s\phi_{kl}}^{\text{SL}}(\mathbf{r}_1, \mathbf{r}_2)$, where one of the hydrogenic functions are replaced by the one-electron radial function,

$$\phi_{E,kl}^{\text{SL}}(r) = \sum_n C_E^{\text{SL}}(1s, nl) R_{nl}(r). \quad (10)$$

The latter numerical radial wavefunction, represents the scattering wavefunction, as obtained through the diagonalization procedure, and contains all the interchannel couplings are represented by the energy dependent coefficients $C_E^{\text{SL}}(1s, nl)$. The obtained numerical wavefunctions $\phi_{E,kl}^{\text{SL}}(r)$ are matched at the boundaries of the box R against the asymptotic expression that an outgoing l electron with momentum k should satisfy, as employed by Burgess [12],

$$\phi_{kl}(r \rightarrow \infty) \rightarrow A \sqrt{\frac{k}{\zeta(r)}} \sin(\delta(r) + \delta_l(k)), \quad (11)$$

with ζ and ϕ function of r , which in the highly asymptotic region satisfy ($r \rightarrow \infty$),

$$\begin{aligned} \zeta(r) &\rightarrow k, \\ \delta(r) &\rightarrow \left[kr + \frac{q_{\text{eff}}}{k} \log(2kr) - \frac{l\pi}{2} + \arg \Gamma \left(l + 1 - i \frac{q_{\text{eff}}}{k} \right) \right], \end{aligned} \quad (12)$$

where $q_{\text{eff}} = 0$, in the present case, is the effective nuclear charge experienced by the outgoing electron and $\delta_l(k)$ is the short-range scattering phase shift. The normalization amplitude A , which represents the usual normalization constant $(2/\pi k)^{1/2}$ in the case of the discretized continuum function, and the scattering short-range phase shift $\delta_l(k)$, are obtained simultaneously after this matching of the numerical scattering radial function and the analytical asymptotic expression (11).

At this point we would like to clarify the limits of the validity of the asymptotic expression (11) that an outgoing electron of angular momentum l and momentum k should satisfy in the case of negative positronium. The extra term, compared to helium or the negative hydrogen, is the mass polarization term $-\nabla_1 \cdot \nabla_2$, whose influence we now examine. In order to separate the radial and angular part of this operator, we write its tensorial form, namely:

$$H_M = -\nabla_1 \cdot \nabla_2 = -\nabla_{r_1} \nabla_{r_2} \mathbf{C}^{(1)}(1) \cdot \mathbf{C}^{(1)}(2), \quad (13)$$

where $\mathbf{C}^{(1)}(i)$, $i = 1, 2$ are renormalized spherical harmonic tensor with components as given by $C_q^{(1)}(\theta, \phi) = \sqrt{4\pi/3} Y_{1q}(\theta, \phi)$, $q = 1, 0, -1$, and ∇_{r_i} , $i = 1, 2$ the one-

electron radial operators,

$$\langle nl | \nabla_{r_i} | n'l' \rangle = \int_0^\infty dr P_{nl} \left[\frac{d}{dr_i} - \frac{l(l+1) - 2 - l'(l'+1)}{2r_i} \right] P_{n'l'}(r), \quad (14)$$

where $l = l' \pm 1$.

Assuming now single-channel ionization into $|1skp\rangle$ continuum, we can see that the value of the matrix element $\langle 1skp | -\nabla_1 \cdot \nabla_2 | 1sk'p \rangle$ depends on the one-electron radial integrals $\langle 1s | \nabla_r | kp \rangle$, $\langle 1s | \nabla_r | k'p \rangle$, which given the bound orbital $P_{1s}(r)$, their values are basically determined in the core region. In this case, one can assume that for such states the asymptotic form (Eq. (11)) may be used for obtaining the correct normalization of the continuum states of negative positronium. The situation, however, is quite different, when the photon energy is sufficient for the excitation of more than one channels. For instance, the interchannel coupling between $|1skp\rangle$ and $|2pk's\rangle$, due to mass polarization term, may not vanish even in the asymptotic region. In this case, a transformation of the Cartesian coordinates $(\mathbf{r}_1, \mathbf{r}_2)$ to Jacobi coordinates [5] is the appropriate one for satisfying the correct asymptotic conditions.

2.3 Photodetachment cross-sections

The transition probability per unit time within lowest non-vanishing order of perturbation theory for non resonant N photon ionization can be written as:

$$W_{fg}^{(N)} = \hat{\sigma}_N I^N, \quad (15)$$

where $\hat{\sigma}_N$ is the total angle-integrated generalized cross-section given by [13]:

$$\hat{\sigma}_N = \pi(2\pi\alpha)^N \Delta E^N \sum_{L_f} \left| D_{L_f}^{(N)} \right|^2, \quad (16)$$

where $\Delta E = \omega(\omega^{-1})$ in the length(velocity) gauge, ω being the photon energy, α being the fine structure constant and $D_{L_f}^{(N)}$ is the N -photon transition amplitude in which the final state is of the form $|SL\rangle$,

$$\begin{aligned} D_{L_f}^{(N)} &\equiv \sum_{\nu_{N-1}} \dots \\ &\times \sum_{\nu_1} \frac{\langle SL_f | D | \nu_{N-1} \rangle \dots \langle \nu_1 | D | g \rangle}{[\omega_g + (N-1)\omega - \omega_{\nu_{N-1}}] \dots [\omega_g + \omega - \omega_{\nu_1}]}, \end{aligned} \quad (17)$$

with D the atomic dipole moment operator that can be expressed either in the length ($D = \mathbf{r}\hat{\mathbf{e}}$, $\hat{\mathbf{e}}$ is the polarization vector) or in the velocity gauge ($D = \hat{\mathbf{e}}\nabla$). The summations are carried over all possible intermediate states including the discrete and continuous parts of the atomic spectrum. The generalization of equation (17) to above threshold detachment of order $N + R$, where N photons

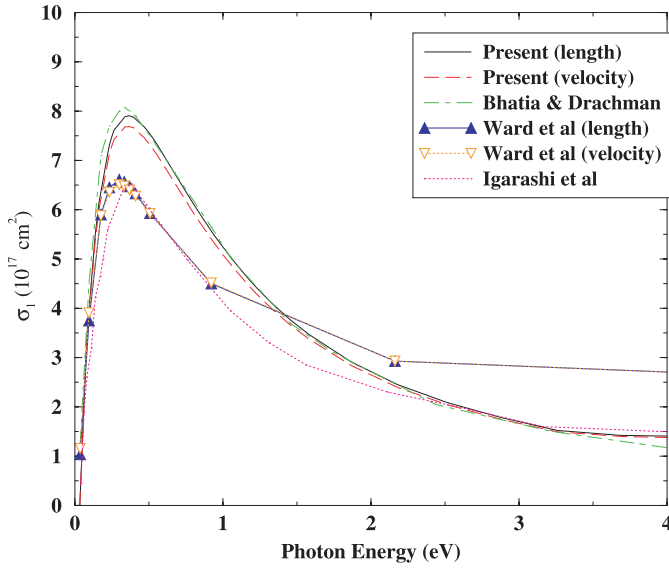


Fig. 1. Photodetachment cross-section in 10^{-17} cm^2 for one photon absorption in both length and velocity gauge.

are needed to ionize the atom plus R extra photons which are absorbed in the continuum, involves the presence of poles in the integral. In that case, equation (17) requires the removal of the poles from the real axis through quantities ϵ_i and taking their limits to zero [14].

The unknown quantities are the $D_{L_f}^{(N)}$ for each ionization channel. In order to calculate the summations over intermediate states in the ATD case, we use the recently developed extrapolation method whose details can be found in [14]. Because of the discretization of the continuum, the detachment rates are calculated for discrete energies. Consequently, these rates in general do not coincide for different channels. For the energy region that we examine, the smoothness and density of data points are sufficient to use a cubic spline interpolation in order to obtain data for intermediate energies.

3 Results

3.1 One-photon detachment

The calculated total one-photon detachment cross-section, as given by equation (16) for $N = 1$, is shown in Figure 1 below a photoelectron energy of 4 eV. Compared with the corresponding spectra for H^- [9], one-photon cross-sections of Ps^- appear qualitatively similar. In particular, in the above figure, the abrupt rising of the cross-section for photon energies near the ionization potential of Ps^- is evident, (as in the case of H^-), in accordance with the Wigner law, $\sigma_l \sim \epsilon^{l+1/2}$, with ϵ being the photoelectron energy. This particular behavior for negative ions originates from the absence of a long range Coulomb potential for the outgoing photoelectron. The cross-section reaches its maximum for photoelectron energy at about 0.34 eV, the ionization potential of Ps^- . For higher energies, but

below the second ionization threshold, the detachment rate decreases gradually as in the case of H^- . The agreement between length and velocity gauge is satisfactory throughout the energy region below the resonances, that begin appearing at 5.1 eV.

Comparing our results with previous works, one photon cross-sections agree very well with those obtained by Bhatia and Drachman [1], using an Hylleras-type wavefunction for the ground state and one-electron active model for the final states. Note that in their study they have plotted the photodetachment cross-sections of Ps^- together with the corresponding results for H^- , which reveals a scaling factor ~ 2 between them. Recently, Igarashi *et al.* [4] used a close-coupling method with a B-spline expansion and calculated the off resonance Ps^- photodetachment cross-sections below the $\text{Ps}(n = 2)$ first ionization threshold. Their results, as well as the cross-sections of one more recent calculation, carried out by Igarashi *et al.* [2] by means of hyperspherical close-coupling method, are in good agreement with the present results below 0.3 eV and above 3 eV. However, they are different up to the cross-section maximum where the cross-section of Igarashi *et al.* is about 15% smaller than the present result. Similar calculations by Ward *et al.* [3], also give a peak value of the one-photon cross-section in agreement with that of Igarashi *et al.*, however they disagree appreciably in higher photon energies, below to $\text{Ps}(n = 2)$ threshold [2].

3.2 Two-photon detachment

For the case of two-photon detachment in the photoelectron energy region (0–1.5 eV), is possible to have one excess photon absorption. From the dipole selection rules, the number of independent channels are two, with final total angular momenta $L = 0, 2$ (*i.e.*, S and D). The order of the process now is higher than for the one photon case and we need to enlarge the atomic basis in order to preserve the reliability of the calculations. The reason for this is that the extrapolation method [14] we use demands a sufficiently high density of states in the energy region where the poles occur. The suitable density of states depends also on the photon energy, independently of the order of the process. Consequently we enlarge the box radius to 450 and at the same time we improve the quality of the B-splines set taking $k = 9$, $N_b = 452$ and a knot sequence that is dense in the energy region close to the nucleus and decreases nearly linearly far away from the nucleus. All calculations have been performed in both the length and velocity gauge and give identical results for the energy region under consideration.

In Figures 2 and 3, we show, for linearly polarized light, the partial photodetachment cross-sections $\sigma^{(2)}(\text{S})$ and $\sigma^{(2)}(\text{D})$ for the S and D waves, respectively. Those cross-sections are defined by [8, 16]:

$$\sigma^{(2)}(i) = \pi(2\pi\alpha)^2 \Delta E^2 |D_{L_i}^{(2)}|^2 \quad L_i = 0, 2. \quad (18)$$

At photoelectron energy 0.19 eV a dip in the detachment cross-section is apparent for the S wave. At this

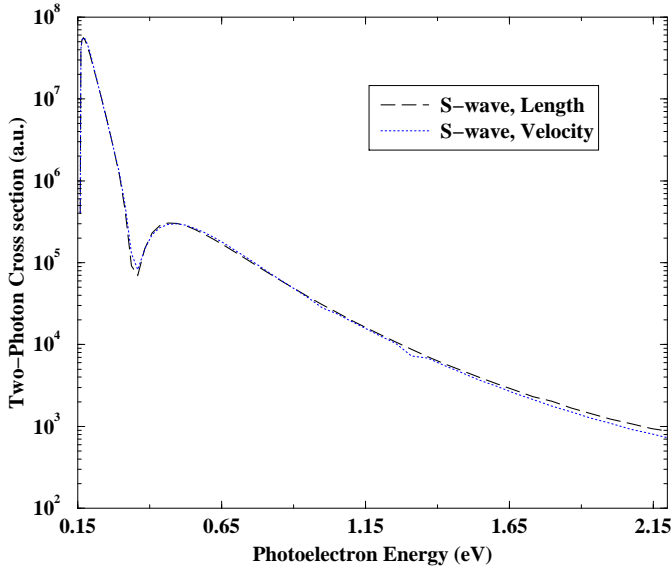


Fig. 2. Photodetachment partial cross-sections in a.u. for S-wave for two photon absorption in length and velocity gauge. Energy region covers detachment with and without ATD, which begins at photoelectron energy ~ 0.19 eV.

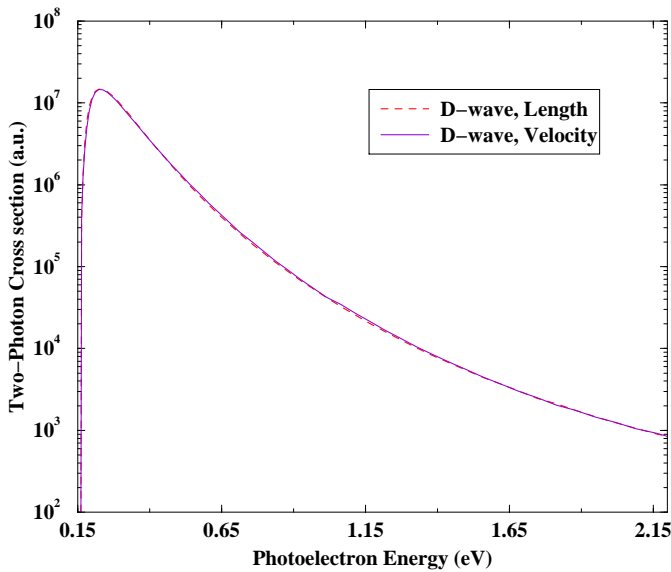


Fig. 3. The same as Figure 2 for D-wave.

photon energy, detachment is allowed with the absorption of one photon only (ATD case) instead of two, and this channel opening gives rise to the increment of the cross-section. This is mostly apparent in the S wave instead of the D wave because of the Wigner threshold law, mentioned previously for the one-photon absorption. A similar in nature dip is reported in the calculation of the two-photon detachment cross-sections by Proulx *et al.* [17] and Nikolopoulos and Lambropoulos [13].

Comparing our results of Ps^- with those of H^- [13], the existence of a scaling factor $\sim 10^2$ is evident. This factor seems to be as expected according to the simple

scaling law between Ps and H [16]:

$$\sigma^{(2)}(i, \omega) = 2^7 \sigma^{(2)}(i, 2\omega) \quad i = \text{S, D} \quad (19)$$

for two-photon detachment ($N = 2$). Of course, here, the contribution of $1/r_{12} - \nabla_1 \cdot \nabla_2$ in the relation (1) should be assumed small enough so as to use the scaling law between Ps and H instead of Ps^- and H^- .

4 Conclusion

While most previous studies were aimed at presenting one-photon cross-sections, the present method enables one to produce results for multiphoton detachment cross-sections. The one-photon cross-sections of Ps^- calculated here, are compared with previous studies as well as with the corresponding spectra for the H^- ion.

Although overall agreement with existing calculations has been found, small but non-trivial differences do appear, undoubtedly due to the differences in the methods of calculation. It seems rather unlikely that differences in the energy of the delicate ground state are the main reason. In any case, this underlines the usefulness of this system as testing ground for methods.

To the best of our knowledge, this is the first study of two-photon detachment cross-sections of the negative positronium ion. Thus, on our attempt to compare our results with previous studies, we assume that the contribution of $1/r_{12} - \nabla_1 \cdot \nabla_2$ in the relation (1) can be neglected, and we use the scaling laws between Ps and H, to compare corresponding results for Ps^- and H^- .

References

1. A.K. Bhatia, R.J. Drachman, Phys. Rev. A **32**, 3745 (1985)
2. I.S.A. Igarashi, N. Toshima, New J. Phys. **2**, 17.1 (2000)
3. S.J. Ward, J.W. Humberston, M.R.C. McDowell, J. Phys. B **20**, 127 (1987)
4. S.N.A. Igarashi, A. Ohsaki, Phys. Rev. A **61**, 032710 (1999)
5. J. Botero, C.H. Greene, Phys. Rev. Lett. **56**, 1366 (1986)
6. N.S. Simonovic, J.M. Rost, Eur. Phys. J. D **15**, 155 (2001)
7. T.N. Chang, R.-Q. Wang, Phys. Rev. A **43**, 1218 (1991)
8. L.B. Madsen, L.A.A. Nikolopoulos, P. Lambropoulos, Eur. Phys. J. D **10**, 67 (2000)
9. X. Tang, T.N. Chang, Phys. Rev. A **44**, 232 (1991)
10. T.N. Chang, X. Tang, Phys. Rev. A **46**, R2209 (1992)
11. T.N. Chang, in *Many-body theory of Atomic Structure* (World Scientific, Singapore, 1993), Chap. B-spline based Configuration-Interaction Approach for Photoionization of Two-electron and Divalent Atoms
12. A. Burgess, Proc. Phys. Soc. Lond. **81**, 442 (1963)
13. L.A.A. Nikolopoulos, P. Lambropoulos, Phys. Rev. A **56**, 3106 (1997)
14. E. Cormier, P. Lambropoulos, J. Phys. B **28**, 5043 (1995)
15. A.M. Frolov, Phys. Rev. A **60**, 2834 (1999)
16. L.B. Madsen, P. Lambropoulos, Phys. Rev. A **59**, 4574 (1999)
17. D. Proulx, M. Pont, R. Shakeshaft, Phys. Rev. A **49**, 1208 (1994)